Development of a multi-layer Cr coating structure model for ATF Cladding and potential incorporation of coating cracking model supported by experimental investigation

Hyuntaek Rho, Youho Lee *
Seoul National University, 1 Gwanak-ro, Gwanak-gu, Seoul 08826, Korea

Corresponding author: leeyouho@snu.ac.kr

***Keywords :** Accident Tolerant Fuel, Cr-coated cladding, Modified Shear-lag Model, Crack density

1. Introduction

As part of the development of Accident Tolerant Fuel (ATF), extensive research is being conducted to enhance high-temperature oxidation resistance by applying chromium (Cr) coatings to the surface of zirconium (Zr) alloy cladding. However, thermo-mechanical loads during reactor operation can induce coating cracking and delamination. These failures lead to localized substrate oxidation, compromising the structural integrity of the cladding. Consequently, it is imperative to establish structural analysis models capable of accurately predicting the mechanical behavior of coated cladding and to elucidate the mechanisms underlying crack initiation. In this study, a multi-layered cladding analysis model based on the two-dimensional Finite Difference Method (FDM) was developed and integrated into the GIFT-1.0, a fuel performance analysis code developed by Seoul National University [1]. Furthermore, this work experimentally observes changes in crack behavior in response to temperature variations and proposes a physical basis for incorporating these findings into the numerical model.

2. Methods and Results

This section describes the development of the 2D FDM-based structural model, the Modified Shear-Lag model, and the experimental observations of temperature-dependent crack formation.

2.1 Development of Structural Analysis Model for Multi-layered Cladding

A structural model based on the 2D FDM was established to calculate the stress distributions of the cladding. This model independently accounts for the material properties of each layer within the multi-layered structure and adopts an incremental formulation to track changes in strain with respect to time increments.

- Equilibrium Equation

In an axisymmetric coordinate system, the equilibrium equation is expressed as follows:

$$\frac{\partial \sigma_{rr}}{\partial r}+\frac{\partial \tau_{rz}}{\partial z}+\frac{\sigma_{rr}-\sigma_{\theta\theta}}{r}=0 \quad \dots (1)$$

$$\frac{\partial \sigma_{zz}}{\partial z}+\frac{\partial \tau_{rz}}{\partial r}+\frac{\tau_{rz}}{r}=0 \quad \dots (2)$$

Where, σ_{rr}, $\sigma_{\theta\theta}$, σ_{zz}, and τ_{rz} represent the radial, hoop, axial, and shear stresses, respectively.

- Incremental Formulation

Nonlinear behavior is numerically resolved by defining the total strain increment as the sum of elastic, plastic, thermal, and creep strain increments:

$$d\epsilon_{total}= d\epsilon_e+d\epsilon_p+d\epsilon_{th}+d\epsilon_{creep} \quad \dots (3)$$

The developed model is currently integrated as a subroutine within the GIFT code, successfully simulating the stress-strain history of the cladding as a function of burnup [1].

2.2 Modified Shear-lag Model

The stress transfer mechanism between the substrate and the coating layer is described by the Modified Shear-lag Model [2-4]. The relationship between strain (ϵ) and crack density (ρ) can be expressed as follows:

$$\rho = \frac{\tau_b}{2Ed_1}\left[\text{Acosh}\left(\text{arsinh}\left(\frac{B}{-A}\right)\right)+\text{Barsinh}\left(\frac{B}{-A}\right)+\epsilon+\frac{\sigma_r}{E}\right]^{-1} \quad \dots (4)$$

with

$$A=\frac{\sigma_b-\sigma_r}{E}-\epsilon,\ B=\tau_b\sqrt{\frac{d_2}{GEd_1}} \quad \dots (5)$$

where τ_b is the interfacial shear strength, E is the elastic modulus of the coating, G is the shear modulus of the interlayer, d_1 and d_2 are the thicknesses of the coating and the interlayer, respectively, and σ_b is the fracture strength of the coating determined by

$$\sigma_b= E\epsilon_0+\sigma_r \quad \dots (6)$$

where ϵ_0 is the initial crack strain and σ_r is the residual stress.

According to Eq. (4), as the strain exceeds a critical threshold, the crack density converges to the saturated crack density (ρ^*) which can be determined as:

$$\rho^*= \frac{\tau_b}{2d_1\sigma_b} \quad \dots (7)$$

2.3 Experimental Procedure

The specimens used in this study were HANA-6 cladding coated with 15 μm-thick Cr layer, machined into a dog-bone geometry. Uniaxial tensile tests were conducted at temperatures ranging from room

temperature (25°C) to the typical PWR operating temperature (330°C). The tests were performed at a constant displacement rate of 0.01 mm/s. The initiation and propagation of cracks as a function of strain were monitored using Digital Image Correlation (DIC), Scanning Electron Microscopy (SEM), and Optical Microscopy (OM). Fig. 1 illustrates the schematic of the dog-bone specimen and the strain distribution captured via DIC. Based on these observations, the relationship between applied strain and crack density was quantified. Particular emphasis was placed on the temperature dependence of the Saturated Crack Density, the point at which crack density remains constant despite further increases in deformation.

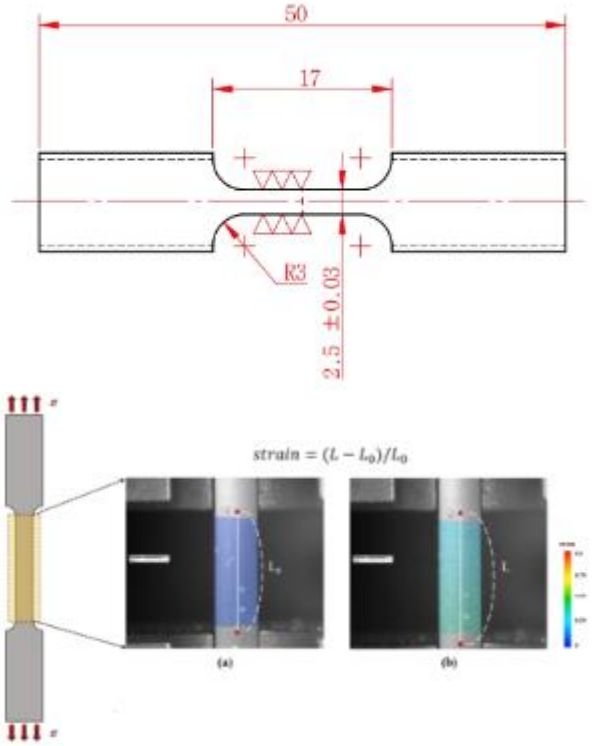

Fig. 1. Schematic of the dog-bone specimen and representative strain distribution map obtained via DIC

2.3 Results and Discussion

The mechanical integrity of the Cr coating was evaluated by comparing experimental data with the predictions of the Modified Shear-lag Model. Fig. 2 shows the evolution of crack density as a function of strain at room temperature, demonstrating good agreement between the experimental results and the model.

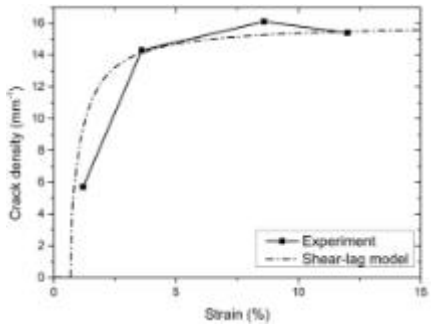

Fig. 2. Evolution of crack density as a function of tensile strain at room temperature (25°C): Comparison between experimental measurements and Modified Shear-lag Model predictions.

A clear correlation was observed between the ambient temperature and the saturation crack density. As shown in Fig. 3, the crack density measured approximately 15 cracks/mm at room temperature (25°C), but significantly decreased as the temperature rose, reaching near-zero values at 200°C.

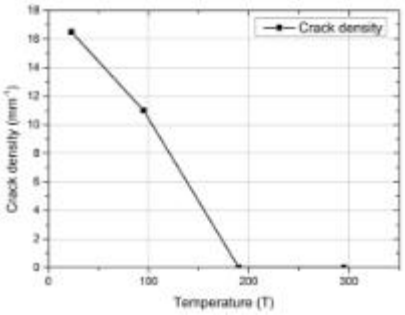

Fig. 3. Temperature dependence of the saturated crack density in Cr-coated HANA-6 cladding, demonstrating a significant reduction in cracking with increasing ambient temperature.

This transition is further evidenced by SEM micrographs in Fig. 4; while numerous channel cracks are visible at 25°C (Fig. 4a), no cracks were observed at 330°C (Fig. 4b) even up to the point of substrate failure.

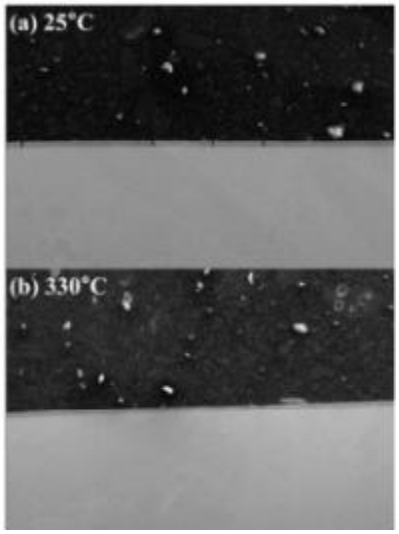

Fig. 4. SEM micrographs of the Cr-coated HANA-6 after tensile failure at different temperatures: (a) at 25°C, and (b) at

330°C

This observed trend is attributed to several interacting mechanisms, primarily starting with the reduction in the yield strength of the HANA-6 substrate at elevated temperatures. Since the interfacial shear strength (τ_b) is proportional to the substrate yield strength, the efficiency of stress transfer from the substrate to the coating is reduced at high temperatures, thereby suppressing crack formation. This is consistent with the well-established linear decrease in Zircaloy yield stress up to 800 K [4], which corresponds to the decrease in τ_b in Eq. (7). Furthermore, the activation of dislocation mobility at high temperatures enhances the fracture toughness of the Cr coating itself. Such an improvement leads to an increase in the critical energy release rate and the initial crack strain (ϵ_0), allowing the coating to accommodate larger deformations before the onset of mechanical failure. In the context of Eq. (6) and (7), this behavior is reflected as an increase in the fracture strength (σ_b) with temperature.

Previous studies on Cr-coated Zircaloy-4 (Zr-4) alloys [4,6] have reported a similar trend, where the crack density decreases as the temperature increases, consistent with the observations in this study. To further validate these findings, the temperature-dependent saturated crack density was analytically calculated using the Modified Shear-lag Model based on established material properties.

According to the Von Mises yield criterion, the interfacial shear strength (τ_b) is typically determined to be at a level comparable to the shear yield strength of the substrate, expressed as $\tau_b \approx \sigma_y / \sqrt{3}$, where σ_y is the yield stress of the matrix. The specific relationship for the yield stress of Zr-4, as detailed in [5], is given by Eq. (8):

$$\sigma_y = \left[\frac{K}{E^n}\left(\frac{\dot{\epsilon}}{10^{-3}}\right)^m\right]^{\left(\frac{1}{1-n}\right)} \quad \ldots (8)$$

where E represents the elastic modulus, K is the strength coefficient, m is the strain rate exponent, and n is the strain hardening exponent, all of which are defined as functions of temperature (T). The yield stress in this study was determined based on a fast neutron fluence of 8×10^{25} n/m^2, a cold work fraction of 0.5, and a strain rate of 0.2 s^{-1}. These conditions are illustrated in Fig. 5(a). Comprehensive equations for each parameter and corresponding graphical data are provided in Ref. [5].

Furthermore, it has been reported in [4] that the initial crack strain (ϵ_0) increases linearly with a shallow slope from 25°C to 450°C, followed by a rapid increase at higher temperatures until cracks virtually disappear near 500°C. Assuming that the temperature-induced variations in the elastic modulus and residual stress have a negligible impact on the cracking behavior, the analytical results are presented in Fig. 5. These results, which include the temperature dependence of (a) yield stress, (b) initial crack strain, and (c) saturated crack density, demonstrate a high degree of consistency with the experimental data reported in [4].

While cracks in HANA-6 disappeared at 200°C, Zr-4 exhibited a trend where cracks vanished at 500°C. This discrepancy may be attributed to differences in coating processes (Arc Ion Plating vs. Magnetron Sputtering), heat treatment conditions (RXA vs. SRA), or alloying elements (Nb in HANA-6 vs. Sn in Zr-4). This remains a subject for further investigation.

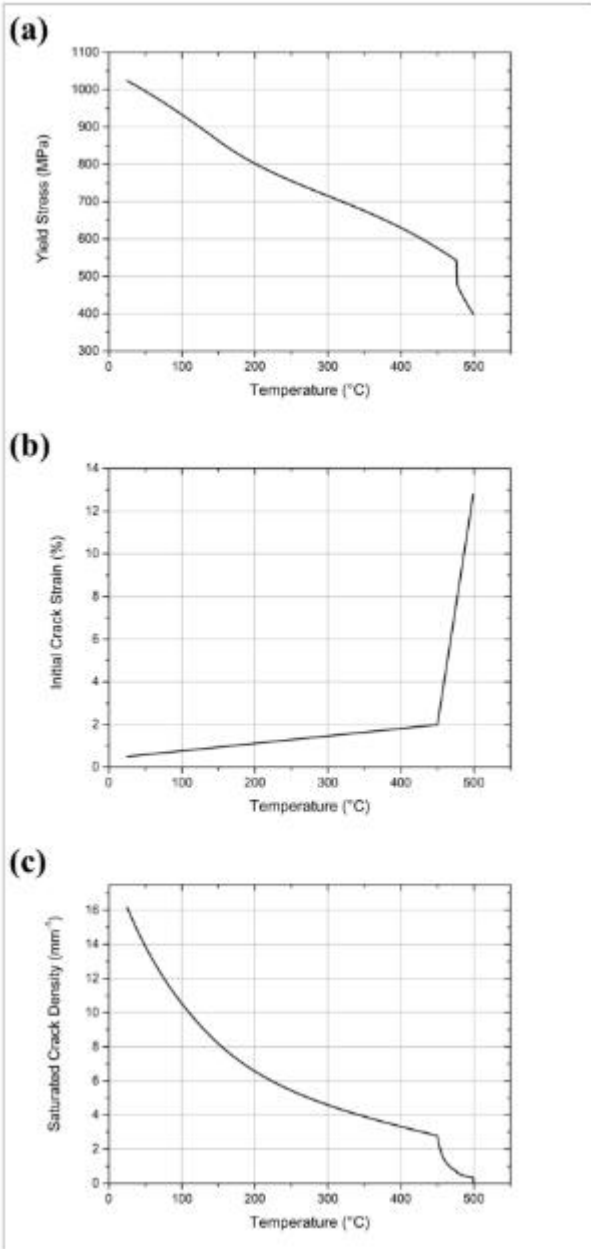

Fig. 5. Analytical prediction of cracking behavior for Cr-coated Zr-4 alloy as a function of temperature: (a) temperature-dependent yield stress of the Zr-4 substrate [5], (b) initial crack strain (ϵ_0) [4], and (c) calculated saturated crack density using the Modified Shear-lag Model.

3. Conclusions

In this study, a two-dimensional finite difference method (FDM)-based model for the structural analysis of multi-layered cladding was developed and successfully integrated into GIFT-1.0, a fuel performance analysis code developed by Seoul National University. The developed model independently accounts for the material properties of each layer and precisely tracks nonlinear deformation behavior over time increments.

Tensile tests conducted on Cr-coated HANA-6 cladding from room temperature to 330°C revealed temperature-dependent cracking behavior, where the saturated crack density decreased sharply with increasing temperature. Specifically, the crack density, which was approximately 15 cracks/mm at room temperature, converged to nearly zero above 200°C. This trend was successfully simulated using the Modified Shear-lag Model. This phenomenon is attributed to the mechanism where the reduction in the yield strength of the HANA-6 substrate at high temperatures lowers the interfacial shear strength, thereby decreasing stress transfer efficiency, combined with the improved ductility and fracture toughness of the Cr coating itself.

Future research will aim to investigate cracking behavior under multiaxial stress conditions that more closely resemble actual reactor environments, moving beyond uniaxial stress states. To achieve this, tensile tests using notched specimens, as well as internal pressure tests and ring tensile tests, will be performed to observe crack initiation and propagation patterns under multiaxial stress. Based on these experimental data, a universal crack model compatible with various temperatures and stress states will be developed. Ultimately, implementing this model into the GIFT code is expected to enhance the performance of cladding integrity assessments by precisely predicting the degree of cracking in accident-tolerant fuel (ATF) and the resulting substrate oxidation behavior.

Acknowledgement

This work was supported by the Korea Institute of Energy Technology Evaluation and Planning(KETEP) and the Ministry of Climate, Energy & Environment(MCEE) of the Republic of Korea (No. RS-2022-KP002856).

REFERENCES

[1] K. Shim, H. Rho, C. Lee, C. Jo, and Y. Lee, GIFT-1.0: Advanced light water reactor fuel performance code, Nuclear Engineering and Technology, Vol. 57, 103567, 2025.

[2] A. P. McGuigan, G. A. D. Briggs, V. M. Burlakov, M. Yanaka, and Y. Tsukahara, An elastic–plastic shear lag model for fracture of layered coatings, Thin Solid Films, Vol. 424, p. 219, 2003.

[3] J. Jiang, H. Zhai, P. Gong, W. Zhang, X. He, X. Ma, and B. Wang, In-situ study on the tensile behavior of Cr-coated zircaloy for accident tolerant fuel claddings, Surface and Coatings Technology, Vol. 394, 125747, 2020.

[4] J. Jiang, H. Zhai, M. Du, D. Wang, X. Pei, X. Ma, and B. Wang, Temperature-dependent deformation and cracking behavior in Cr coating for accident tolerant fuel cladding: An in situ SEM study, Surface and Coatings Technology, Vol. 427, 127815, 2021.

[5] K. J. Geelhood, C. E. Beyer, and W. G. Luscher, PNNL stress/strain correlation for Zircaloy, Pacific Northwest National Laboratory (PNNL), Richland, WA, No. PNNL-17700, 2008.

[6] Y. Taïbi, A. Charbal, J. C. Brachet, E. Rouesne, S. Sao-Joao, S. Kalacska, J. Michler, and G. Kermouche, High temperature chromium coating cracking investigation during tensile tests monitored by acoustic emission, Journal of Nuclear Materials, Vol. 605, 156108, 2025.